TELKOMNIKA Indonesian Journal of Electrical Engineering
Vol.12, No.7, July 2014, pp. 5003 ~ 5010
DOI: 10.11591/telkomnika.v12i7.4259

Three-Dimensional Thermal Analysis of Three-Phase Enclosed GIS Bus Bars

Li Hongtao, Shu Naiqiu, Li Ling*
School of Electrical Engineering, Wuhan University
No.8, Donghunan Road, Hongshan District, Wuhan 430072, China
*Corresponding author, e-mail: 5pro@163.com

Abstract

The ampacity of GIS bus bars is limited by the maximum operation temperature of the contacts. This paper employs the coupled eddy current, fluid and thermal finite-element method (FEM) to solve the three-dimensional (3-D) heat transfer problem in a three-phase enclosed GIS bus bar. The contact resistance is considered and described as a resistor between the conductor and the contact finger. In order to avoid convective boundary condition on the tank surface which is not easy to apply, the ambient air is introduced into the solution region. The temperature dependent thermal properties of SF_6 gas and air are considered. The temperatures calculated by proposed model are found to be in good agreement with the experimental data of a 126 kV three-phase enclosed bus bar prototype.

Keywords*: GIS bus bar, contact resistance, finite-element method (FEM), temperature rise*

1. Introduction

Gas insulated switchgear (GIS) is one of the paramount components in power systems. Once failures happen, huge metropolitan areas will suffer the loss of power supply, affecting the reliability of power system and leading to large economic loss and negative social impact. Overheat caused by contact degradation is one of the most frequent failures in GIS. The contact resistance becomes larger than normal value after contact degradation occurs, which increases the contact temperature and will worsen the contact condition. Contact degradation is a self-accelerated process that after a long period of gradual increasing contact resistance escalates rapidly, causing local melting and finally leading to short circuit failure [1-3]. Thus, in order to avoid catastrophic fault, knowledge of the temperature rise in GIS bus bar is quite necessary after it has been put into service.

Over the years, substantial efforts have been devoted to the thermal modeling of GIS bus bars. Models based on coupled two-dimensional (2-D) finite-element-analytic technique have been proposed to predict temperature rise in GIS bus bars [4-7]. Three-dimensional (3-D) models based on the finite-element method (FEM) are used to study the temperature distribution of the bus duct systems [8, 9]. However, in these papers the convective heat transfer coefficient is an empirical parameter and hard to be determined especially when the structure investigated is complicated. Moreover, the contact resistance has to be considered because it always makes the contact the hottest part in GIS bus bar.

In order to calculate the temperature rise in GIS bus bars, a 3-D finite element model is established to solve the coupled eddy current, fluid and thermal problem. For better accuracy, the variation of fluid thermal peoperties with temperature is considered. The contact resistance is described as a resistor between the conductor and the contact. The ambient air is introduced into the solution region to avoid the convective boundary condition on the tank surface. The proposed model is applied on a 126 kV three-phase enclosed GIS bus bar prototype and validated by the temperature rise experiment.

2. Solution Region and Finite Element Mesh

The solution region of the electromagnetic field and thermal analysis is given in Figure 1. Because of the multi-scale of different components in GIS bus bar and the existence of

Received August 29, 2013; Revised March 15, 2014; Accepted March 26, 2014

surrounding air in the solution region, the computation scale is increased. Appropriate mesh quality is necessary to ensure the convergence of iteration process in CFD analysis. The solution region is meshed with 4,924,540 elements and 3,964,038 nodes. Finite element mesh of the air, the conductor, the tank and the SF_6 gas is shown in Figure 2. Table 1 and Table 2 give, respectively, the main geometrical data and material properties of the analyzed model.

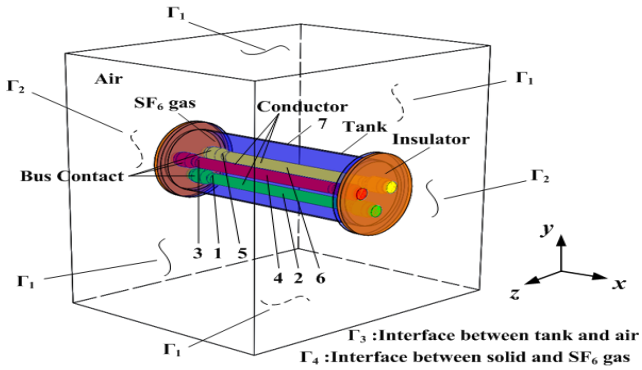

Figure 1. Solution Region of Thermal Analysis

Table 1. Main Geometry Data of the GIS Bus Bar Model (mm)

Components	Outer diameter	Inner diameterThickness	Length
Conductor	85	65	1200
Tank	508	492	1500

Table 2. Material Data of the Model at 0℃

Components	Density(kg/m^3)	Thermal conductivity (10^{-2} W/(m·K))	Dynamic viscosity (10^{-5} Pa·s)	Specific heat (J/(kg·K))
SF_6 gas	22.82	1.206	1.42	665.18
Air	1.293	2.44	1.72	1005
Conductor	2730	220	–	880

(a) Air (b) Conductor and tank (c)SF_6 gas

Figure 2. Mesh of the Solution Region

3. Three-Dimentional Eddy Current Field Model

Temperature rise of the bus contact is higher than that of the conductor because of the contact resistance. Therefore, the power loss in contact region must be considerd in the thermal analysis. For the case of plum blossom contact, the contacts are located between the insulator and conductor, which is equalized to a resistor R located between the bulk resistance of contact finger R_f and the conductor R_c, as shown in Fig. 3. The simplification is deemed to be

reasonable for further thermal analysis because the heat capacity of the contact is small. In this paper, the contact resistance is considered to be temperature dependent by [10]:

$$R = R_0(1+\frac{2}{3}\alpha\Delta\theta) \tag{1}$$

Where R_0 is the contact resistance at room temperature, α is the coefficient of resistivity, $\Delta\theta$ is the temperature difference.

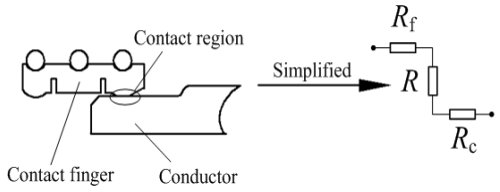

Figure 3. Schematic of the Contact Resistance

The following assumptions are used in the analysis process: displacement current is neglected because of the low frequency; the current flowing in the conductor is sinusoidal; the reluctivity is taken as constant. Introducing the magnetic vector potential $\boldsymbol{A}$ and the electric scalar potential Φ into Maxwell's equation, the equations governing 3-D eddy current field can be written as [8]:

$$\begin{cases} \nabla\times(\nu\nabla\times\boldsymbol{A})-\nabla(\nu\nabla\cdot\boldsymbol{A})=\boldsymbol{J}_t \ \text{ in V} \\ \nabla\cdot(-\sigma(T)\dfrac{\partial\boldsymbol{A}}{\partial t}-\sigma(T)\nabla\phi)=0 \qquad \text{in V}_1 \end{cases} \tag{2}$$

$$\boldsymbol{J}_t=\boldsymbol{J}_s+\boldsymbol{J}_e=\boldsymbol{J}_s-\sigma(T)\frac{\partial\boldsymbol{A}}{\partial t}-\sigma(T)\nabla\phi \tag{3}$$

Where V is the whole solution region, V_1 is the eddy current region, T is the temperature, t is the time, σ is the conductivity, ν is the reluctivity, $\boldsymbol{J}_t$, $\boldsymbol{J}_e$ and $\boldsymbol{J}_s$ are, respectively, the total current, eddy current and source current density.

Joule heat loss P_c in the conductor and eddy current loss P_t in the enclosure are expressed as:

$$P_c=\frac{1}{2}\int_V\frac{|\dot{\boldsymbol{J}}_s|^2}{\sigma(T)}dv \tag{4}$$

$$P_t=\frac{1}{2}\int_V\frac{|\dot{\boldsymbol{J}}_e|^2}{\sigma(T)}dv \tag{5}$$

Assuming the outer boundary of the solution region is far away from the GIB. The boundary condition on Γ_1 is:

$$\boldsymbol{A}|_{\Gamma_1}=\boldsymbol{0} \tag{6}$$

Boundary Γ_2 is a symmetrical boundary of which the magnetic induction is 0 in *y*- and *z*-axis directions. The boundary condition on Γ_2 is expressed as:

$$A_y|_{\Gamma_B}=A_z|_{\Gamma_B}=0 \tag{7}$$

4. Three-Dimentional Thermal Model

Convection and radiation are the most influential heat transfer mechanism because the heat generated in GIS bus bar gets dissipated mainly by convection and radiation to the surroundings. The solution region and finite element mesh of eddy-current field and CFD analysis is identical, thus power losses can be mapped into thermal field by the element with the same number. Unlike the traditional FEM in which the convection boundary condition is needed and the heat transfer coefficient on the tank surface is viewed as constant, an air domain outside the GIS bus bar has also been modeled for simulating the heat transfer by convection and radiation to the surroundings. The natural convection both inside and outside the GIS bus bar are solved with the CFD theory. The steady-state governing equations for CFD analysis are employed as follows [11-13]:

Continuity equation:

$$\nabla \cdot (\rho \boldsymbol{V}) = 0 \tag{8}$$

Momentum equation:
x-axis direction:

$$\nabla \cdot (\rho u \boldsymbol{V}) = -\frac{\partial p}{\partial x} + \nabla \cdot (\mu \nabla u) \tag{9}$$

y-axis direction:

$$\nabla \cdot (\rho v \boldsymbol{V}) = -\frac{\partial p}{\partial y} + \nabla \cdot (\mu \nabla v) + \rho f_y \tag{10}$$

z-axis direction:

$$\nabla \cdot (\rho w \boldsymbol{V}) = -\frac{\partial p}{\partial z} + \nabla \cdot (\mu \nabla w) \tag{11}$$

Energy equation:

$$\nabla \cdot (\rho C T \boldsymbol{V}) = \nabla \cdot (\lambda \nabla T) + Q_{\mathrm{v}} \tag{12}$$

Where ρ, λ and μ are, respectively, the density, thermal conductivity, and dynamic viscosity, $\boldsymbol{V}$ is gas velocity, u,v and w are, respectively, the velocity components in x-, y- and z-axis directions, p is the gas pressure, $\boldsymbol{I}$ is the identity matrix, C is the specific heat, Q_v is the volumetric heat source, f_y is the gravitational acceleration in *y*-axis direction, T is Kelvin temperature.

Proper boundary conditions are necessary for thermal analysis of GIS bus bar. In the external air domain, air is treated as ideal gas. Constant temperature boundary condition is applied on the outmost boundary of air domain, stated as:

$$T|_{\Gamma_1} = T_{\mathrm{a}} \tag{13}$$

Where T_a is the ambient temperature.

Non-slip boundary conditions are applied on Γ_1 , Γ_3 and Γ_4:

$$V_x = V_y = V_z = 0 \tag{14}$$

There is radiation heat transfer between the conductors and tank and between the tank and surrounding air. Thermal radiation heat transfer has large effects on the overall temperature rise of GIS bus bar, especially when the temperature difference increases and the convection is natural. Because the heat flow that causes radiation varies with the fourth power of the absolute temperature, the thermal analysis considering radiation is highly nonlinear. The radiation effects

generally appear in the heat transfer analysis only through the boundary conditions. Two types of radiation boundary conditions are used in the model. On the outer tank surface (Γ_3), an open type enclosure surface radiation boundary condition is applied as follows:

$$-\lambda \frac{\partial T}{\partial n}|_{\Gamma_3} = \varepsilon\sigma(T^4 - T_a^4) \tag{15}$$

Where n is the normal direction of tank surface, ε is emissivity, σ is Stefan-Boltzmann constant,.

Between the outer surface of the conductors and the inner surface of the tank (Γ_4), a closed type enclosure surface radiation is considered. Each radiating surface is characterized with an emissivity and the same enclosure number assigned to it. The formulation of this boundary condition is expressed as [14];

$$-\lambda \frac{\partial T}{\partial n}|_{\Gamma_4} = \varepsilon F_{ij}\sigma(T_i^4 - T_j^4) \tag{16}$$

Where T_i and T_j are the temperatures of the radiating two surfaces, F_{ij} is the view factor, which can be obtained by the following equation:

$$F_{ij} = \frac{1}{A_i}\iint_{A_i A_j} \frac{\cos\theta_i \cos\theta_j}{\pi r^2} dA_i dA_j \tag{17}$$

Where A_i and A_j are areas of the two surfaces, r is the distance between the two surfaces, θ_i and θ_j are the polar angles formed by the radiation line and the normal of the two surfaces.

Finally, adiabatic boundary condition is adopted and the gas velocity in the x-axis direction is 0 on Γ_2, stated as:

$$-\lambda \left.\frac{\partial T}{\partial n}\right|_{\Gamma_2} = 0, \quad V_x = 0 \tag{18}$$

In order to ensure solution accuracy of the thermal model, the thermal physical properties except the specific heat of the SF_6 gas and air are considered to be temperature dependent in the CFD analysis. The density variation with the temperature and pressure is evaluated by the ideal gas law.

$$\rho = \rho_0 \frac{pT_0}{p_0 T} \tag{19}$$

The thermal conductivity and viscosity of gas are nearly not influenced by gas pressure. Their variation with temperature is obtained by Sutherland's law [15].

$$\lambda = \lambda_0 \left(\frac{T}{T_0}\right)^{1.5} \frac{T_0 + S}{T + S} \tag{20}$$

$$\mu = \mu_0 \left(\frac{T}{T_0}\right)^{1.5} \frac{T_0 + S}{T + S} \tag{21}$$

Where ρ_0, λ_0 and μ_0 are, respectively, the density, thermal conductivity and dynamic viscosity of the SF_6 gas and air at 0℃, S is the Sutherland temperature, T_0 and p_0 are the reference temperature and pressure, respectively.

Adiabatic boundary condition is adopted and the gas velocity in the x-axis direction is 0 on boundary Γ_2, stated as:

$$-\lambda \left.\frac{\partial T}{\partial n}\right|_{\Gamma_2} = 0, \quad V_x = 0 \tag{21}$$

5. Results and Discussions

5.1. Power Losses

The numerical simulation is carried out with ANSYS 12.0. The power losses in GIS bus bar are caused by both current flowing in the conductors and eddy current induced in the tank. Because the contact resistance is temperature dependent, the eddy current and thermal fields are solved iteratively. Firstly, the initial temperatures are assumed in the contacts and the other components of GIS bus bar. Then, the initial temperatures are continually updated until the error between the calculated temperature and the initial value is less than 5%. Assuming the contact resistance of each phase to be 20 μΩ, the eddy current distribution in the tank of GIS bus bar at rated current 2000 A is given in Figure 4. The power losses in the three-phase conductors and in the contacts of the GIS bus bar are 342.95 W and 51.31 W, respectively.

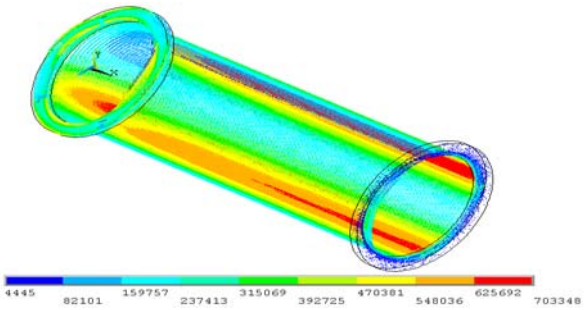

Figure 4. Eddy Current Distribution on the Tank Surface

5.2. Temperature Distribution

The pressure of SF_6 gas is 0.35MPa. The calculated power losses are used as heat source in the CFD analysis. Steady-state conjugate heat transfer analysis isconducted at the ambient temperature 25℃. The temperature distribution of GIS bus bar under the current of 2000 A is shown in Figure 5. The maximum temperature locates at the contacts and the conductors of phase A and C have nearly identical temperature distributions. The contact temperature of phase B is 87.2℃, and that of phase A and C is 91.7℃. This is attributed to the symmetric spatial locations of phase A and C, and the flow characteristics of heated SF_6 gas, which moves upwards under the effect of buoyancy and brings heat to the upper parts of GIS bus bar. The convective heat transfer coefficient on the tank surface is calculated with Newton's law of cooling. The distribution is given in Figure 6. The *x*- and *y*-directions are shown in Figure 3. The heat transfer coefficient is proved to be variable at different locations on the tank surface. The maximum value is 4.5W/(m^2·K) at the position of *y*=0. Large discrepancy exists between the maximum value and the minimum one.

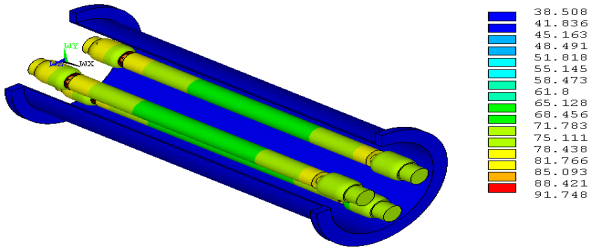

Figure 5. Temperature Distribution of the GIS Bus Bar

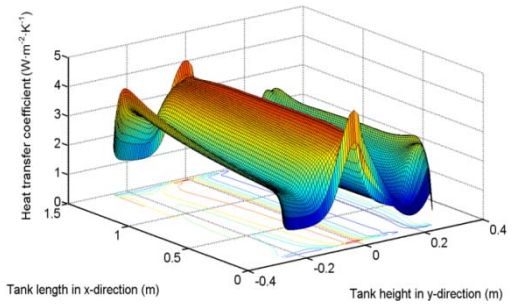

Figure 6. Heat Transfer Coefficient Distribution on the Outer Tank Surface

5.3. Laboratory Tests

In order to check the accuracy of the proposed methodology, laboratory tests are conducted on a 126kV GIS bus bar prototype, which is shown in Figure 7. The temperatures are measured with Pt100 temperature sensors, which are installed on the tank surface, on the contact of each phase, and on the middle of the conductors. The ambient temperature is also measured with a sensor installed 2 meters away from the GIS bus bar. Considering the environmental factor, N_2 gas with the pressure of 0.4MPa is substituted for SF6 gas. The conductors are connected in series and fed with a current source. Before the experiment, the contact resistance of each phase is measured. The contact resistance of phase A, phase B, and phase C are, respectively, 42.6μΩ, 43.8μΩ, and 44.2μΩ. Comparison between the tested and calculated temperature rises at different load currents is given in Table 3. The measurement points are shown in Figure 1. It is founded that the contact temperature rises are higher than those of other components in GIS bus bar, and the temperature difference becomes more obvious as the current increases. The calculated temperature rises are in good agreement with the tested results.

Figure 7. Experimental Set-up of the 126kV Three-phase GIS Bus Bar

Table 3. Comparison of the Simulated and Tested Temperature Rises (K)

Measurement points	Current *I*=1000 A		Current *I*=1980 A	
	Simulated	Tested	Simulated	Tested
1	17.7	15.9	54.1	46.6
2	16.4	15.2	49.4	43.7
3	18.1	18.2	54.6	51.8
4	16.9	17.2	50.0	49.3
5	18.0	17.8	54.7	52.5
6	16.7	17.0	50.0	48.9
7	5.9	5.3	17.1	16.0

4. Conclusion

Contact resistance has to be considered in the thermal analysis of three-phase enclosed GIS bus bars. In this paper, the contact resistance is simplified to be a resistor

between the conductor and the contact finger in the solid model. The ambient air is also introduced into the solution region to avoid the convective boundary condition on the tank surface. The 3-D FEM is used to solve the coupled eddy current, fluid and thermal problem. The model proposed is validated with the test results on a 126kV GIS bus bar prototype. The model is helpful in determining the contact temperature in GIS bus bar.

References

[1] Runde M, Lillevik O, Larsen V. Condition assessment of contacts in gas-insulated substations. *IEEE Transactions on Power Delivery*. 2004; 19(2): 609-617.

[2] Mukaiyama Y, Takagi I, Izumi K. Investigation on abnormal phenomena of contacts using disconnecting switch and detachable bus in 300 kV GIS. *IEEE Transactions on Power Delivery*. 1990; 5(1): 189-195.

[3] Mukaiyama Y, Takagi I, Izumi K. Contact-failure phenomena and their development in gas-insulated switchgear. *Electrical Engineering in Japan*. 1993; 113(2): 733-740.

[4] Hwang CC, Chang JJ, Jiang YH. Analysis of electromagnetic and thermal fields for a bus duct system. *Electric Power Systems Research*. 1998; 45(1): 39-45.

[5] Hedia H, Henrotte F, Meys B, et al. Arrangement of phase and heat constraints in a bus bar. *IEEE Transactions on Magnetics*. 1999; 35(3):n1274-1277.

[6] Kim JK, Hahn SC, Park KY. Temperature rise prediction of EHV GIS bus bar by coupled magnetothermal finite element method. *IEEE Transactions on Magnetics*. 2005; 41(5): 1636-1639.

[7] Kim SW, Kim HH, Hahn SC. Coupled finite-element-analytic technique for prediction of temperature rise in power apparatus. *IEEE Transactions on Magnetics*. 2002; 38(2): 921-924.

[8] Ho SL, Li Y, Lin X. Calculations of eddy current, fluid, and thermal fields in an air insulated bus duct system. *IEEE Transactions on Magnetics*. 2007; 43(4): 1433-1436.

[9] Ho SL, Li Y, Lin X. A 3-D study of eddy current field and temperature rises in a compact bus duct system. *IEEE Transactions on Magnetics*. 2006; 42(4): 987-990.

[10] Paulke J, Weichert H, Steinhaeuser P. Thermal simulation of switchgear. *IEEE Transactions on Components and Packaging Technologies*. 2002; 25(3): 434-439.

[11] Rajagopala K, Panduranga V, Lunavath H. Computation of electric field and thermal properties of 3-phase cable. *TELKOMNIKA Indonesian Journal of Electrical Engineering*. 2012; 10(2): 265-274.

[12] Wu XW, Shu NQ, Li HT. Thermal analysis in gas insulated transmission lines using an improved finite-element model. *TELKOMNIKA Indonesian Journal of Electrical Engineering*. 2013; 11(1): 458-467.

[13] Lee SH, Lee BY, Kim HK. Local heat source approximation technique for predicting temperature rise in power capacitors. *IEEE Transactions on Magnetics*. 2009; 45(3): 1250-1253.

[14] Eteiba MB, Aziz AMM, Shazly JH. Heat conduction problems in SF_6 gas cooled-insulated power transformers solved by the finite element method. *IEEE Transactions on Power Delivery*. 2008; 23(3): 1457-1463.

[15] Anderson JD. *Computational Fluid Dynamics*. New York: McGraw-Hill. 1995.